Supplemental Material

Rationale for targeting mitochondrial metabolism in pancreatic cancer

Pancreatic adenocarcinoma (PDAC) is defined by a number of hallmarks: high rate of *KRAS* activating and *TP53* inactivating mutations, propensity for local and distant invasion, desmoplasia resulting in a hypovascular and hypoxic microenvironment, reprograming of cellular metabolism, and tumor immune invasion.[1-4] These characteristics are regarded to be downstream events of metabolic reprogramming.[5] Metabolic reprogramming is an emerging hallmark of PDAC, including aerobic glycolysis, oxidative phosphorylation (OXPHOS), glutaminolysis, lipogenesis and lipolysis, autophagic status, and anti-oxidative stress. However, accumulating evidence has revealed that plasticity is another feature of PDAC metabolism, in which each cancer cell remodels biochemical pathways of energy transduction and associated anabolism in response to various stresses.[6] Both intrinsic factors (such as the *KRAS*, *MYC*, *TP53*, *CDKN2A* and *SMAD4* genes) and extrinsic factors (such as microenvironment – desmoplasia, hypoxia, immune suppression) regulate metabolic plasticity.[7]

The intrinsic factors for metabolic plasticity induce abnormal mitochondrial metabolism and enhance glycolysis, with alterations in glutamine and lipid metabolism. The extrinsic factors induce cancer cells to reprogram their metabolic pathway and hijack stromal cells (mainly cancer-associated fibroblasts and immunocytes) to communicate, thereby adapting to metabolic stress. This provides a strong rationale for novel therapies that target the mitochondrial metabolism.[8]

Figure 1. CPI-613 inhibits mitochondrial metabolism selectively in tumor cells[9,10]

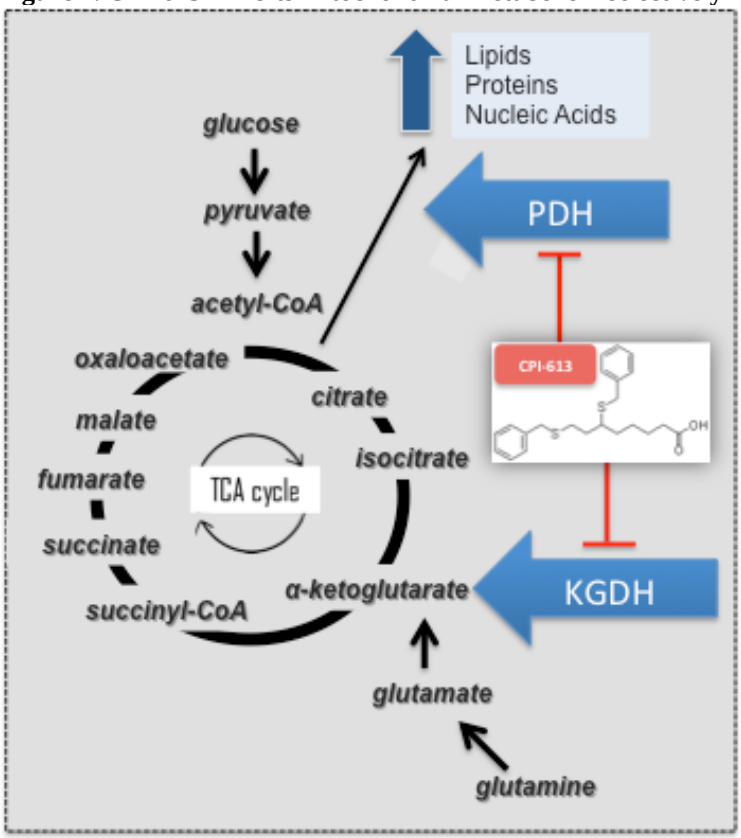

Drug inhibition of the tumor cell TCA cycle substantially reduces the mitochondrial export of anabolic intermediates, including those essential to nucleotide synthesis. Compromised nucleotide synthesis is expected to substantially interfere with the efficiency of the DNA damage response. In turn, the DNA damage response is necessary for tumor cells to resist and recover from the effects of the active FOLFIRINOX components.

Pharmacokinetics

CPI-613 (6,8-bis-benzylsulfanyloctanoic acid) is rapidly converted within minutes by beta-oxidation to the active metabolite (4,6-bis-benzylsulfanyloctanoic acid) (CPI-2850). In model systems, CPI-2850 is similar in potency to CPI-613. In study 57112, the pharmacokinetics of CPI-613 and the metabolite CPI-2850 were evaluated in 18 patients treated at 500 mg/m^2 and in 2 patients treated at 1000 mg/m^2, following either a short (14-20 mins) or long IV infusion 2hrs). Plasma samples for PK analysis were collected pre-dosing with CPI-613 and at approximately 5, 30, 60, 90 mins, 2, 4, 6, 8, 24 and 72 hrs post infusion.

Non-compartmental PK data analysis (NCA) was conducted using a validated installation of WinNonLin v6.4 (Pharsight Corp, CA). The PK parameters of CPI-613 and CPI-2850, together with their summary statistics are presented in Table 1. The observed pharmacokinetics of CPI-613 are consistent with the results of a prior escalating dose Phase I study in patients with advanced hematologic malignancies.[11]

As shown in Figure 2, CPI-613 and CPI-2850 follow a bi-phasic disposition profile with the emergence of secondary peaks best seen in the levels of CPI-613 in graph B during the elimination phase, indicative of possible entero-hepatic recirculation. The only major metabolite identified in plasma was CPI-2850 and no glucuronide and sulfoxide metabolites were observed. The biotransformation of CPI-613 occurred rapidly following infusion, with CPI-2850 becoming the major circulating species in plasma over time.

Figure 2. Mean pharmacokinetic profile of CPI-613 and the active metabolite CPI-2850 in plasma following a single IV infusion (500-1000 mg/m^2) in patients.

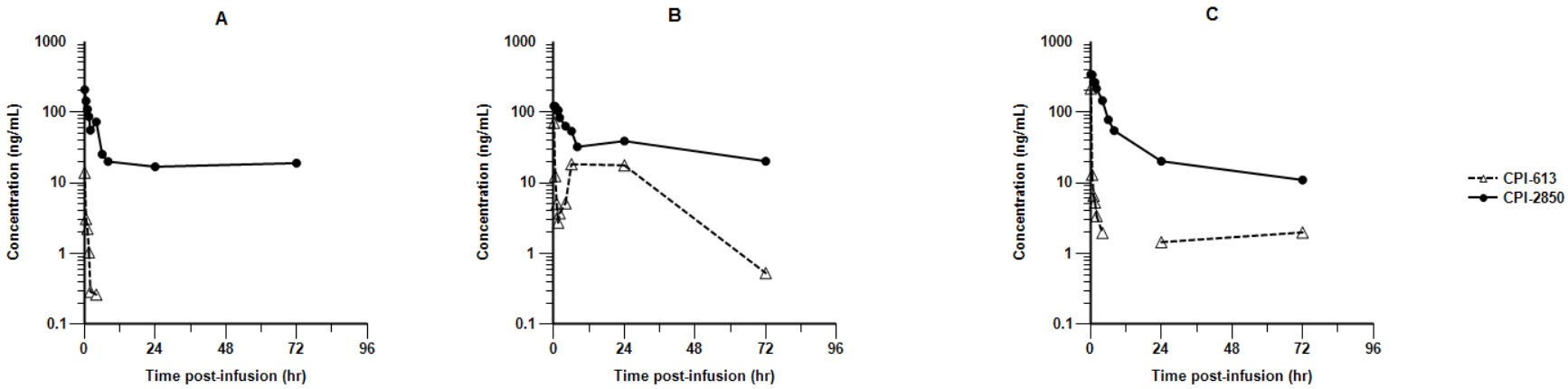

A. 500 mg/m^2 (Long Infusion; 2hrs N=6 patients); B. 500 mg/m^2 (Short Infusion; 14 to 20 mins N=12 patients); C. 1000 mg/m^2 (Long Infusion; 2hrs N=2 patients).

Table 1. CPI-613 and CPI-2850 Pharmacokinetic Parameter Estimates in Plasma Following a Single IV Infusion (500-1000 mg/m^2); Short Infusion (14 to 20 mins); Long Infusion (2 hrs)

CPI-613 Dosage (mg/m^2)	Analyte	Infusion Duration*	Statistics	T_{max} (hr)	C_{max} (ng/ml)	AUC_{last} (hr*ng/ml)	$t_{1/2}$ (hr)
500	CPI-613	Short	N	12.00	12.00	12.00	2.00
			Mean	4.86	85.51	654.26	0.52
			CV%	189.57	53.69	215.85	22.49
			Min	0.36	5.97	2.67	0.44
			Median	0.41	82.66	70.90	0.52
			Max	24.30	162.47	4831.97	0.61
500	CPI-613	Long	N	6.00	6.00	6.00	3.00
			Mean	2.08	13.90	20.60	9.74
			CV%	0.00	107.10	102.15	150.26
			Min	2.08	4.80	7.46	0.60
			Median	2.08	6.92	11.33	2.00
			Max	2.08	43.46	62.46	26.61
500	CPI-2850	Short	N	12.00	12.00	12.00	10.00
			Mean	1.73	160.20	2710.91	50.54
			CV%	103.72	42.59	95.21	65.86
			Min	0.36	60.46	469.61	6.96
			Median	0.83	166.36	2104.76	44.96
			Max	6.30	267.43	10406.11	117.26
500	CPI-2850	Long	N	6.00	6.00	6.00	5.00
			Mean	2.73	230.81	2105.89	78.23
			CV%	58.55	38.49	30.62	73.01
			Min	2.08	154.11	1621.91	16.29
			Median	2.08	215.14	1957.53	53.71
			Max	6.00	400.71	3367.96	160.20

CPI-613 Dosage (mg/m^2)	Analyte	Infusion Duration*	Statistics	T_{max} (hr)	C_{max} (ng/ml)	AUC_{last} (hr*ng/ml)	$t_{1/2}$ (hr)
1000	CPI-613	Long	N	2.00	2.00	2.00	2.00
			Mean	2.08	215.27	353.56	34.18
			CV%	0.00	125.49	109.18	6.81
			Min	2.08	24.25	80.61	32.53
			Median	2.08	215.27	353.56	34.18
			Max	2.08	406.30	626.51	35.82
1000	CPI-2850	Long	N	2.00	2.00	2.00	2.00
			Mean	2.29	373.35	3009.31	16.71
			CV%	12.97	34.95	29.69	82.75
			Min	2.08	281.07	2377.46	6.93
			Median	2.29	373.35	3009.31	16.71
			Max	2.50	465.63	3641.16	26.48

Figure 3. Incidence of neuropathy

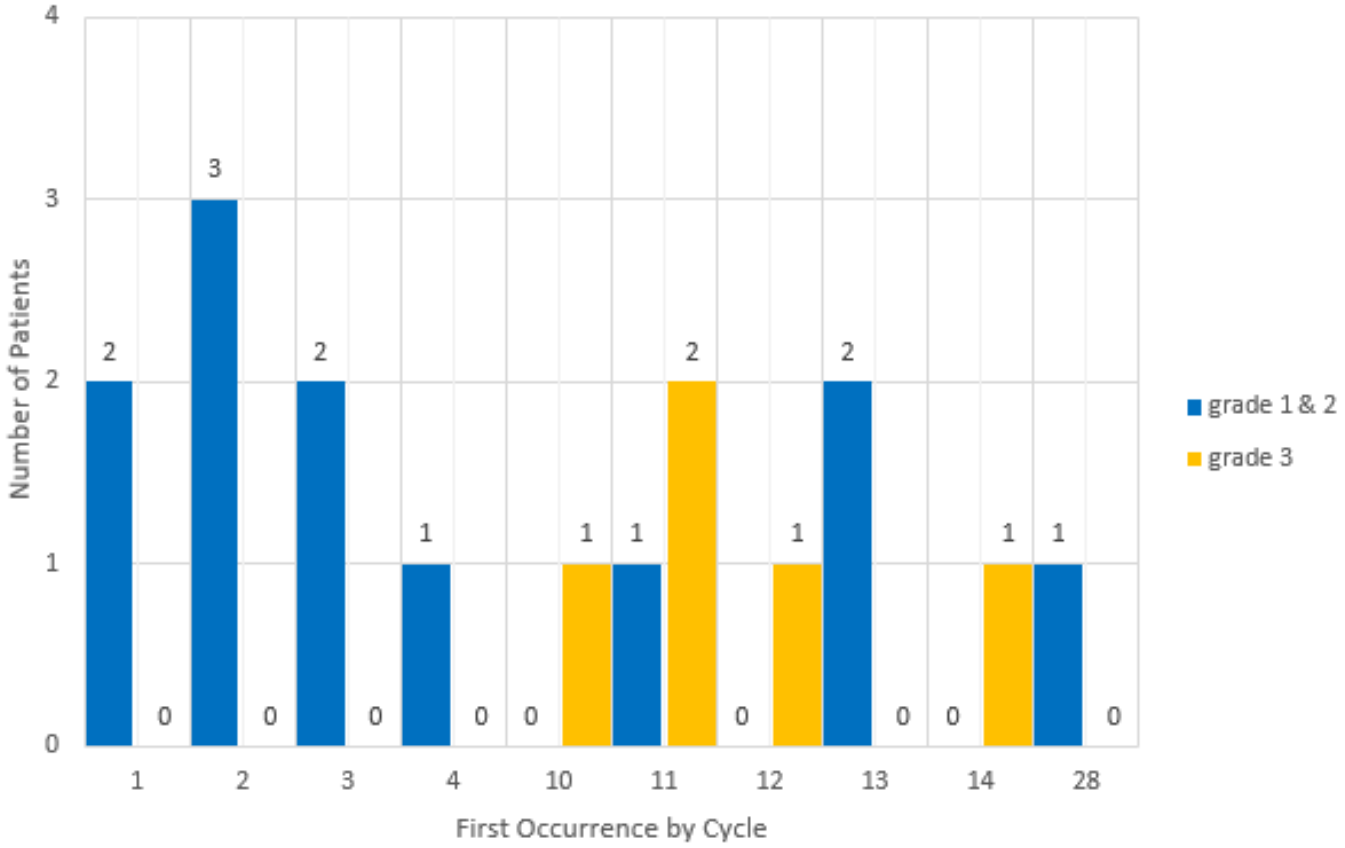

Whole Exome Genomic DNA Sequencing of the Three CPI-613 Responders

In order to gain insight into the genetic features associated with the complete responses to the combined treatment by CPI-361 and FOLFIRINOX, tumor tissues and matching peripheral blood samples from three available exceptional responsive patients, CPI-ER1, CPI-ER2, and CPI-ER3, were obtained from Wake Forest Baptist Comprehensive Cancer Center Tumor Tissue Bank. Genomic DNAs were isolated and subjected to whole exome DNA sequencing (75x75 bp paired ends) on an Illumina NextSeq 500 using the Illumina TruSeq Rapid Exome Library prep kit. Tumor DNA samples were sequenced to an average depth of 300X and the matching normal DNA samples were sequenced to an average of 50X.

The raw fastq files were generated by four different lanes using the illumina TruSeq Rapid Exome Library. For each fastq file, it was aligned to reference (hg19) by BWA mem,[12] with version bwa-0.7.12. The preprocessing for somatic mutation calling includes duplicate mark by Picard (https://broadinstitute.github.io/picard/), indel realignment by GATK 3.6 (https://software.broadinstitute.org/gatk/), and base recalibration by GATK 3.6. This preprocessing was implemented for each sam output from BWA. For each sample, the four aligned bam files were merged as the final bam by Samtools 1.3.1,[13] after adding read group (RG) information into each aligned bam file during preprocessing. The somatic mutation calling was implemented by MuTect1-1.1.4,[14] VarScan2 -2.3.9,[15] and Somatic-SNIPER.[16] The somatic mutation loci and genes for each sample were combined from the outputs of the three pipelines for somatic mutation calling. To specify the tumor purity for the VarScan2, we utilized AbsCN-seq software.[17] The estimated tumor purities were compared with those from pathologists (**Table 2**).

Table 2. Tumor purities for tumor samples of CPI-613 responders

Sample	AbsCN-seq	Pathologist
CPI-ER1	0.36* or 0.38	~40%
CPI-ER2	0.41* or 0.46	~30%
CPI-ERS	0.46 or 0.56	~30%*

*The value was selected for tumor-purity parameter of VarScan2

Using the above three pipelines for somatic mutation calling, we identified 219, 1,999, and 135 somatically mutated genes in samples of CPI-ER1, CPI-ER2, and CPI-ER3, respectively. The mutation rates were comparable with those reported PDAC cohorts (**Table 3**). Mutations in *KRAS*, *TP53*, and *SMAD4* genes are known to be commonly mutated in PDACs in most published cohorts including TCGA,[18] ICGC,[19] paad_utsw_2015,[20] and paad_qcmg_uq_2016.[21] In our three responders, *KRAS* mutations were found in all three cases and *TP53* mutations were found in two cases. Interestingly, *SMAD4* mutation was not found in any of the three responders. In addition, our analysis revealed frequent mutations in the members of mucin gene family including *MUC4*, *MUC12*, *MUC17*, *MUC20*, *MUC22*, and *MUC5B* (T**ables 4**). Whereas mucin genes have been found to be mutated in PDACs, the frequencies are much lower than what we found in the three responders to CPI-613 and FOLFIRINOX (**Table 4**). SMAD3/SMAD4 has been shown to act as a transcriptional factor for *MUC4*, which is regulated by TGF signaling. Therefore, *MUC* gene mutations may represent a common defect in the TGF pathway in a subset of PDACs and this alteration may result in a vulnerability to the combination treatment targeting genome and mitochondria-associated metabolism. Consistent with this hypothesis, some MUC family members have been shown to locate to the mitochondria[22] and be regulated by hypoxia.[23] Future functional studies are needed to shed light on this potentially important mechanism of targeted therapeutics for PDACs.

Table 3. Statistics of somatic mutated loci and genes from MuTect1, VarScan2, and Somatic-Sniper

Callers	CPI-613 responders		
	CPI-ER1	CPI-ER2	CPI-ER3
MuTect1	1,906	9,099	1,491
VarScan2 (indels)	214	422	194
VarScan2 (SNPs)	2,310	4,144	1,555
Somatic-SNIPER	910	732	851
Total loci #	4,481	13,220	3,275
Genes #	219	1,999	135

Table 4. Mutation genes with their distributions in public cohorts and CPI-613 responders

Mutated genes	Our Samples			Public Cohorts*			
	CPI-ER1	CPI-ER2	CPI-ER3	paad_qcmg_uq_2016 383 samples	paad_utsw_2015 109 samples	paad_tcga 186 samples	paad_icgc 99 samples
KRAS	X	X	X	90%	92%	91%	95%
TP53	X	X		66%	50%	69%	33%
SMAD4				22%	19%	25%	16%
MUC17	X	X	X	1.60%	6%	4%	1%
MUC4		X		4%	6%	2%	2%
MUC12	X	X		0.80%	0%	0%	0%
MUC20	X			0%	1.80%	0%	0%
MUC22	X	X		0.80%	0%	0%	0%

MUC5B	X	1.30%	9%	2%	1%

*Source data were downloaded from cBioPortal and the mutations are validated.

Comparison with FOLFIRINOX alone at our institution

We sought and obtained IRB exemption to perform the search. We queried the hospital Electronic Medical Record Epic's Clarity Relational Database for primary diagnosis codes of malignant neoplasm of pancreas (ICD-10 C25 and ICD-9 157) between January 1, 2012 and December 1, 2016. There were 1145 patients matching the criteria. Then, we queried Epic to identify how many of those 1145 patients received FLUOROURACIL and the result was 90 patients. Next, we excluded 25 patients who received CPI-613 for this study (CCWFU 57112) or for compassionate use. For the remaining 65 patients, Irinotecan and Oxaliplatin administration dates and doses, vitals, last contact, race, and ethnicity were retrieved from Epic. The Cancer Registry has been utilized for staging and previous treatments for those patients including surgery, radiation therapy etc. In order to validate and complete the data that had been extracted from Epic and the Cancer Registry, we performed a chart review of 65 patients and excluded patients who would not have met criteria such as non-stage IV, neoadjuvant therapy etc. 6 patients were excluded due to pancreatic adenocarcinoma not being the primary diagnosis. 29 patients were not diagnosed with stage IV disease at presentation. 8 patients were excluded because they were not treated with FOLFIRINOX in the front line setting. 22 patients have been identified and validated with stage IV pancreatic adenocarcinoma at diagnosis and who were treated with FOLFIRINOX in the first line setting. In addition, we documented their ECOG performance status at diagnosis, date of diagnosis, and treatment response. Each patient's chart was independently reviewed by two different physicians to ensure the accuracy of the reported findings (Figure 4).

Figure 4. Kaplan-Meier estimates of patients treated with FOLFIRINOX-CPI-613 combination and FOLFIRINOX alone during the same time period at the study's institution

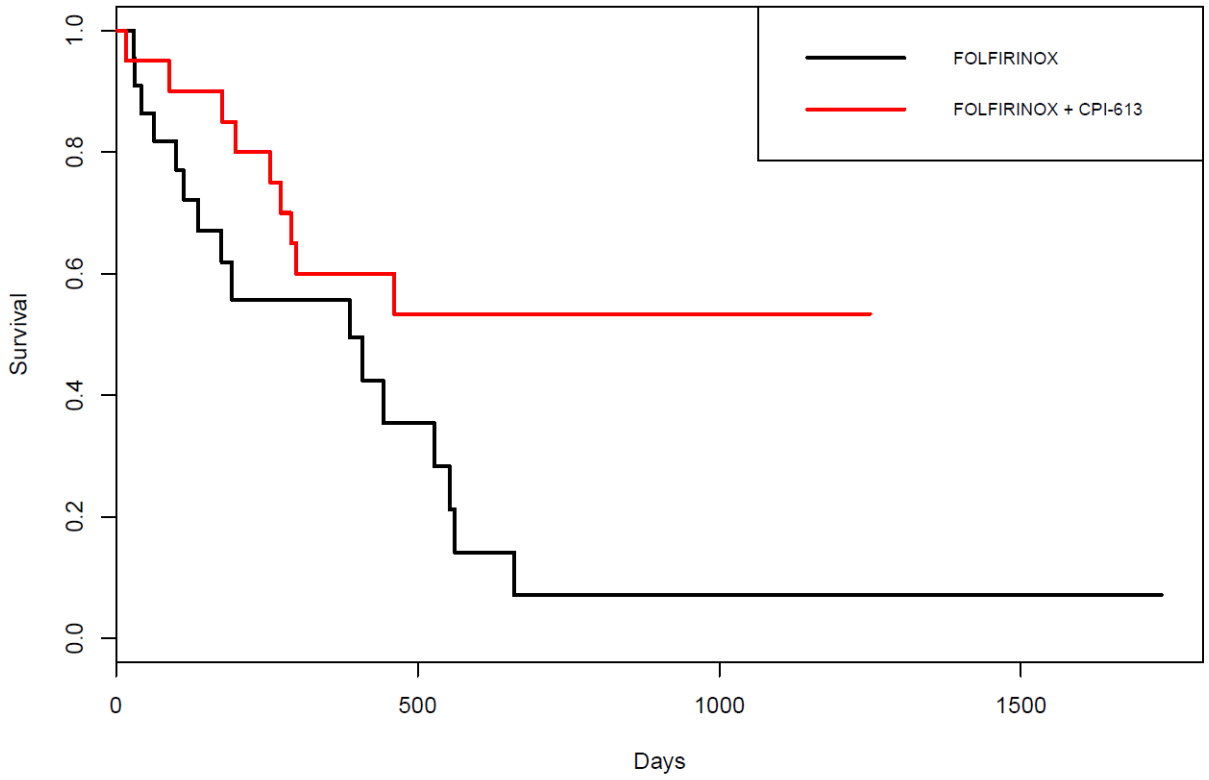

Table 5. Summary of adverse events[1] by event over the course of 233 cycles (patients can have multiple toxicities), n = 18 participants

Toxicity	Grades 1-2[2]	Grade 3	Grade 4
Anemia	208	5	0
Hyperglycemia	155	39	1
Platelet count decreased	179	3	0
Peripheral sensory neuropathy	155	8	0
Alkaline phosphatase increased	162	0	0
Fatigue	93	4	0
Hypoalbuminemia	82	0	1
Hypomagnesemia	78	0	0
Diarrhea	69	7	0
Lymphocyte count decreased	53	16	0
Pain	59	0	0
Aspartate aminotransferase increased	57	0	0
Nausea	52	2	0
Hyponatremia	47	3	0
Hypokalemia	31	9	1
Alanine aminotransferase increased	37	0	0
Anxiety	37	0	0
Anorexia	32	2	0
Weight loss	30	1	0
White blood cell decreased	27	0	0
Hypertension	24	1	0
Abdominal pain	20	4	0
Dysgeusia	24	0	0
Constipation	22	0	0
Edema limbs	22	0	0
Gastrointestinal disorders - Other	19	0	0
Chronic kidney disease	18	0	0
Hypocalcemia	18	0	0
Depression	15	2	0
Vomiting	11	3	0
Cough	13	0	0
Insomnia	12	0	0
Skin and subcutaneous tissue disorders - Other	12	0	0
Dizziness	10	0	0
General disorders and administration site conditions - Other	8	1	0
Hypophosphatemia	5	4	0
Neutrophil count decreased	4	4	1

Toxicity	Grades 1-2[2]	Grade 3	Grade 4
Back pain	7	1	0
Dehydration	5	3	0
Dyspnea	7	1	0
Thromboembolic event	4	3	0
Chills	6	0	0
Sinus tachycardia	6	0	0
Urinary tract infection	6	0	0
Ventricular arrhythmia	5	1	0
Cardiac disorders - Other	3	2	0
Fever	4	1	0
Hypoglycemia	5	0	0
Pleural effusion	5	0	0
Activated partial thromboplastin time prolonged	4	0	0
GGT increased	3	1	0
Gastroesophageal reflux disease	4	0	0
Generalized muscle weakness	4	0	0
Leukocytosis	0	4	0
Malabsorption	4	0	0
Myalgia	4	0	0
Rash maculo-papular	4	0	0
Urinary frequency	4	0	0
Weight gain	4	0	0
Ascites	3	0	0
Atelectasis	3	0	0
Blood bilirubin increased	3	0	0
Flatulence	3	0	0
Headache	3	0	0
Mucositis oral	3	0	0
Non-cardiac chest pain	3	0	0
Pericardial effusion	3	0	0
Proteinuria	3	0	0
Bloating	2	0	0
Blurred vision	2	0	0
Bruising	2	0	0
Creatinine increased	2	0	0
Dysphagia	1	1	0
Edema face	2	0	0
Fall	2	0	0
Flashing lights	2	0	0

Toxicity	Grades 1-2[2]	Grade 3	Grade 4
Flushing	2	0	0
Hyperhidrosis	2	0	0
Hypernatremia	2	0	0
Hypertriglyceridemia	2	0	0
Hypoxia	1	1	0
Nasal congestion	2	0	0
Palpitations	2	0	0
Papulopustular rash	2	0	0
Productive cough	2	0	0
Psychiatric disorders - Other	2	0	0
Renal hemorrhage	2	0	0
Respiratory, thoracic and mediastinal disorders - Other	2	0	0
Urinary tract pain	2	0	0
Vascular disorders - Other	2	0	0
Catheter related infection	0	1	0
Enterocolitis infectious	0	1	0
Esophageal infection	0	1	0
Glucose intolerance	0	1	0
Infections and infestations - Other	0	1	0
Lung infection	0	1	0
Pancreatitis	0	1	0
Sepsis	0	0	1

[1] There were no grade 5 toxicities
[2] For incidence greater than 10%

References

1. Feig C, Gopinathan A, Neesse A, et al. (2012). The pancreas cancer microenvironment. Clin Cancer Res, 18(16), 4266-4276.
2. Chiarugi P and Cirri P. Metabolic exchanges within tumor microenvironment. Cancer Lett. 2016 Sep 28;380(1):272-80.
3. Neesse A, Michl P, Frese KK, et al. Stromal biology and therapy in pancreatic cancer. Gut. 2011 Jun;60(6):861-8.
4. Wang M, Chen MY, Guo XJ, et al. Expression and significance of HIF-1α and HIF-2α in pancreatic cancer. J Huazhong Univ Sci Technolog Med Sci. 2015 Dec;35(6):874-9.
5. Wei H, Li F, Fu P, et al. Effects of the silencing of hypoxia-inducible Factor-1 alpha on metastasis of pancreatic cancer. Eur Rev Med Pharmacol Sci. 2013 Feb;17(4):436-46.
6. Seyfried TN, Flores RE, Poff AM, et al. Cancer as a metabolic disease: implications for novel therapeutics. Carcinogenesis. 2014 Mar;35(3):515-27.
7. Obre E and Rossignol R. Emerging concepts in bioenergetics and cancer research: metabolic flexibility, coupling, symbiosis, switch, oxidative tumors, metabolic remodeling, signaling and bioenergetic therapy. Int J Biochem Cell Biol. 2015 Feb;59:167-81.
8. Liang C, Qin Y, Zhang B, et al. Metabolic plasticity in heterogeneous pancreatic ductal adenocarcinoma. Biochim Biophys Acta. 2016 Sep 4;1866(2):177-188.
9. Zachar Z, Marecek J, Maturo C, et al. Non-redox-active lipoate derivates disrupt cancer cell mitochondrial metabolism and are potent anti-cancer agents in vivo. J Mol Med. 2011; 89: 1137-48.
10. Stuart SD, Schauble A, Gupta S, et al. A strategically designed small molecule attacks alpha-ketoglutarate dehydrogenase in tumor cells through a redox process. Cancer Metab. 2014 Mar;2(1):4.
11. Pardee TS, Lee K, Luddy J, et al. A phase I study of the first-in-class antimitochondrial metabolism agent, CPI-613, in patients with advanced hematologic malignancies. Clin Cancer Res. 2014 Oct 15;20(20):5255-64.
12. Li H, Durbin R. Fast and accurate short read alignment with Burrows-Wheeler transform. Bioinformatics 2009; 25: 1754-1760.
13. Li H, Handsaker B, Wysoker A, et al. Genome Project Data Processing S. The Sequence Alignment/Map format and SAMtools. Bioinformatics 2009; 25: 2078-2079.
14. Cibulskis K, Lawrence MS, Carter SL, et al. Sensitive detection of somatic point mutations in impure and heterogeneous cancer samples. Nat Biotechnol 2013; 31: 213-219.
15. Koboldt DC, Zhang Q, Larson DE, et al. VarScan 2: somatic mutation and copy number alteration discovery in cancer by exome sequencing. Genome Res 2012; 22: 568-576.
16. Larson DE, Harris CC, Chen K, et al. SomaticSniper: identification of somatic point mutations in whole genome sequencing data. Bioinformatics 2012; 28: 311-317.
17. Bao L, Pu M, Messer K. AbsCN-seq: a statistical method to estimate tumor purity, ploidy and absolute copy numbers from next-generation sequencing data. Bioinformatics 2014; 30: 1056-1063.
18. Cancer Genome Atlas. Comprehensive molecular characterization of human colon and rectal cancer. Nature 2012; 487: 330-337.
19. Biankin AV, Waddell N, Kassahn KS, et al. Pancreatic cancer genomes reveal aberrations in axon guidance pathway genes. Nature 2012; 491: 399-405.
20. Witkiewicz AK, McMillan EA, Balaji U, et al. Whole-exome sequencing of pancreatic cancer defines genetic diversity and therapeutic targets. Nat Commun 2015; 6: 6744.
21. Bailey P, Chang DK, Nones K, et al. Genomic analyses identify molecular subtypes of pancreatic cancer. Nature 2016; 531: 47-52.
22. Moniaux N, Chaturvedi P, Varshney GC, et al. Human MUC4 mucin induces ultra-structural changes and tumorigenicity in pancreatic cancer cells. British Journal of Cancer 2007; 97: 345-357.
23. Joshi S, Kumar S, Ponnusamy MP, et al. Hypoxia-induced oxidative stress promotes MUC4 degradation via autophagy to enhance pancreatic cancer cells survival. Oncogene 2016; 35: 5882-5892.